ISBN: 978-3-95450-231-8 ISSN: 2673-5490 doi: 10.18429/JACoW-IPAC2023-TUPA138

CHARACTERISATION OF A Cs – IMPLANTED Cu PHOTOCATHODE

L. A. J. Soomary[1*], C. P. Welsch[1], Department of Physics, University of Liverpool, UK
L. B. Jones[1†], R. Valizadeh[1], T. C. Q. Noakes[1], ASTeC, STFC Daresbury Laboratory, UK
[1] also at the Cockcroft Institute, Sci-Tech Daresbury, Warrington, UK

Abstract

The generation of high–brightness electron beams is a crucial area of particle accelerator research and development. Photocathodes which offer high levels of quantum efficiency when illuminated at visible wavelengths are attractive as the drive laser technology is greatly simplified. The higher laser power levels available at longer wavelengths create headroom allowing use of manipulation techniques to optimise the longitudinal and transverse beam profiles, and so minimise electron beam emittance. Bi–alkali photocathodes which offer quantum efficiency ∼ 10% under illumination at 532 nm are an example of this. Another solution is the use of modified photoemissive surfaces. Caesium has a low work function and readily photoemits when illuminated at green wavelengths (∼ 532 nm). Caesium oxide has an even lower work function and emits at red wavelengths (∼ 635 nm). We present data on our work to create a hybrid copper photocathode surface modified by implantation of caesium ions, measuring the surface roughness and probing its structure using MEIS. We measure the energy spread of photoemitted electrons, the QE as a function of illumination wavelength, and the practicality of this surface as a photocathode by assessing its lifetime on exposure to oxygen.

INTRODUCTION

The most crucial parameters describing photocathode performance are quantum efficiency (QE), mean transverse energy (MTE), and operational lifetime (τ). These factors in turn define the ultimate electron beam performance which is measurable as normalised emittance, and minimising beam emittance duly maximises beam brightness. There are many strategies to improve these parameters, but understanding and influencing the relevant cathode surface physics underpinning these parameters and their co–dependence is the focus of photocathode engineering and R&D.

Attributes such as work function (ϕ) and surface roughness (R_a) define a cathode's primary photoemission characteristics. A high level of surface roughness may increase photon absorption and thereby quantum efficiency (QE), but will also increase the energy spread of photoemitted electrons. Similarly, a low work function may increase QE, but at the expense of increased energy spread and so worsened beam brightness [1]. The interplay between different photocathode properties is subtle [2], with an improvement in one area of parameter space often adversely affecting another. Operational robustness is arguably the most important consideration for a practical photocathode, and it is for this reason that polycrystalline metals are widely used as photocathode electron sources in particle accelerators [3–5]. Such metals typically have low QE and require high–power laser illumination at UV wavelengths (Ti:Sapp, 3rd harmonic) to drive electron emission. Operational lifetime is impacted by the vacuum conditions with residual gases forming new composites on the photocathode surface, changing its chemistry and workfunction [6, 7]. This has been shown to drive a progressive reduction in QE for semiconductor [8], alkali–metal [9] and single–crystal metal photocathodes [10].

The performance of metal photocathodes can be modified in several ways. Micro–machining of the surface to increase photon absorption and improve electron emission has been shown to improve QE [11], as has the application of ultra–thin metal oxide films [12]. Lifetime may be improved by applying a protective barrier layer on the cathode surface such as a metal oxide film [12] or graphene [13]. We seek to manufacture a photocathode based on a metal surface modified through Cs ion implantation at low energy (< 1 keV), thereby boosting QE and shifting the photoemission threshold to longer wavelengths. This potentially reduces the size and complexity of the drive laser, also reducing the incident laser power and the detrimental effect of surface heating [14] whilst facilitating the application of sophisticated modification techniques to the transverse laser pulse profile [15], thereby minimising electron beam emittance and maximising beam brightness. Previously Cs ion implantation has been investigated at high energy (25 & 400 keV) [16–18].

EXPERIMENTAL DETAILS

Experiments were performed on 6 mm diameter polycrystalline Cu pucks supplied by Surface Preparation Laboratory, with measured surface roughness $R_a < 30$ nm. On receipt, the Cu pucks were cleaned with acetone in an ultrasonic bath for 20 minutes, then mounted in cathode holders compatible with the Scienta Omicron 19 mm flag system [19]. Each mounted Cu puck was then loaded into our Multiprobe system [20], and subjected to repeated cycles of argon ion bombardment (15 minutes) and annealing at 550 °C (60 minutes) until clean XPS spectra were obtained.

Samples were transferred between the Multiprobe and PPF (III–V Photocathode Preparation Facility) [21] using a UHV/XHV vacuum suitcase, so excellent vacuum conditions (∼ 10^{-10} mbar) were maintained throughout. The TESS and PPF are connected together, so XHV vacuum conditions were maintained during transfers between these systems. Prior to Cs ion implantation, we measured a series of transverse energy distribution curves (TEDC) using our TESS facility [22] to establish baseline levels of mean transverse energy (MTE) for the un–modified Cu pucks.

* liam.soomary@liverpool.ac.uk
† corresponding author – lee.jones@stfc.ac.uk

ISBN: 978-3-95450-231-8 ISSN: 2673-5490 doi: 10.18429/JACoW-IPAC2023-TUPA138

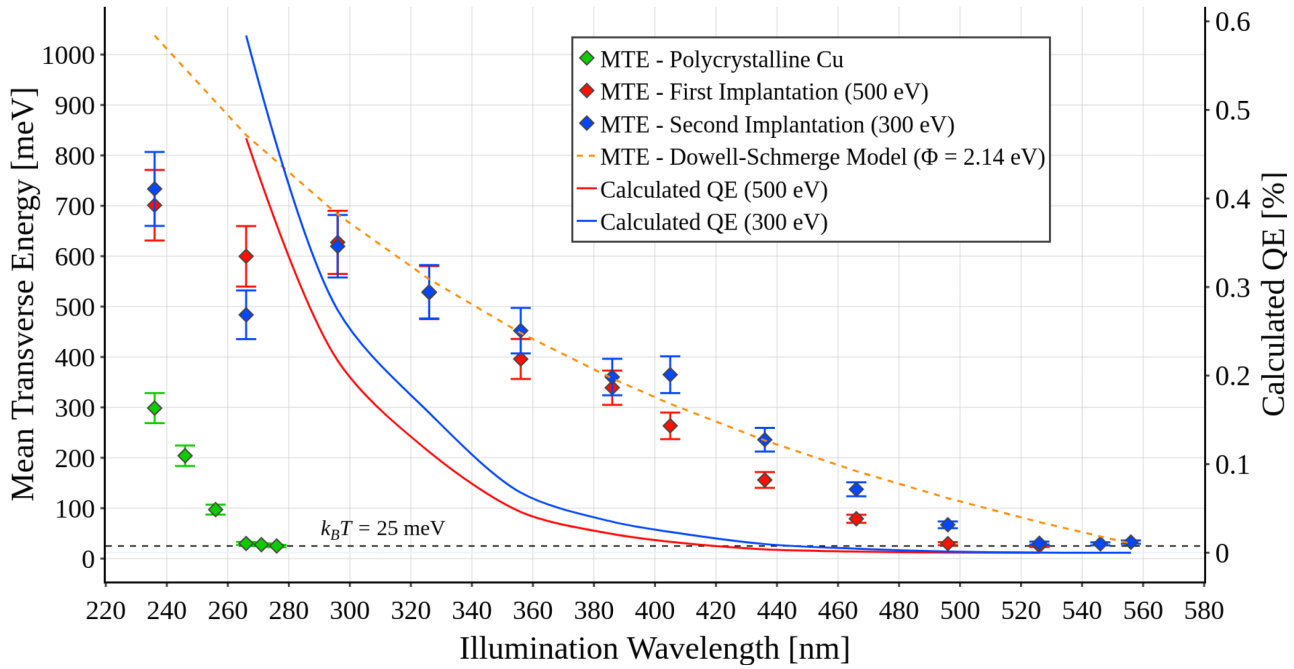

Figure 1: MTE and calculated QE values as a function of the illumination wavelength for a pure Cu sample (**green**), after a first ion implantation cycle at 500 eV **(red)**, and a second ion implantation cycle at 300 eV **(blue)**. The **orange** dashed line shows the Dowell–Schmerge MTE estimate based on a published value for the Cs work function [24]. The thermal floor at room temperature given by k_BT = 25 meV is shown by the black dashed line.

We used a Hiden HAL IG5c high–brightness Cs ion source designed for secondary ion mass spectroscopy (SIMS) to carry out Cs ion implantation. This was installed on the cleaning chamber of our PPF. The Cu puck was held on the PPF magnetic linear translation arm (MLTA) during ion implantation. The MLTA is is not electrically isolated, so we installed a Z–translation stage with a 'calibration plate' connected to a picoammeter to measure the ion flux from the Cs source. We established ion source settings to maintain a drain current of 500 nA at ion kinetic energies of 300 eV and 500 eV. The calibration plate was then retracted and the sample moved into position with the MLTA rotated to orientate the sample surface normal towards the ion source during implantation.

Several Cs–implanted Cu samples were prepared using a recipe based on two 1–hour Cs ion exposures, the first involving Cs–implantation at 500 eV and the second at 300 eV. The output from the IG5c source is predominantly Cs^{1+} ions, so each 1–hour exposure equates to around 11.2×10^{15} ions. After implantation, QE at 405 nm was measured in the PPF storage chamber. Tests were then carried out on each sample to determine the nature of the photoemissive surface and to characterise their electron emission.

The first Cs–implanted Cu sample was transferred to the TESS vacuum chamber for TEDC/MTE measurements [22] after the initial 500 eV implantation, with further TEDC/MTE measurements made following the subsequent 300 eV implantation. The results of this are summarised in Fig. 1. On completion of photoemission characterisation in the TESS, this sample was moved back to the Multiprobe (using the vacuum suitcase) for an additional QE measurement at 266 nm, and work function with thermal decomposition. The second sample was subjected to progressive degradation by O_2 exposure in the TESS, with the effect of this gas exposure on QE measured.

Using a combination of the measured photoemission image intensity in the TESS, the detector gain and the measured optical power illuminating the photocathode, we calculated the trend in QE and fitted this between the measured values at 266 nm and 405 nm. This is shown in Fig. 1.

Additionally, we carried out Medium Energy Ion Scattering using the MEIS facility at the University of Huddersfield [25] to establish the Cs ion implantation depth.

RESULTS

Fig. 1 summarises our results for the first sample, showing the MTE after both the first and second implantation steps. For comparison, we also show the measured MTE for clean copper prior to ion implantation. The work function of clean copper (4.65 eV [24]) is clearly much higher than that of the Cs–implanted Cu, with the MTE commensurately reduced and emission at the 25 meV thermal floor when the illumination wavelength reaches around 270 nm. The first stage of Cs ion implantation has a substantial effect on the photoemissive properties of this system, with a huge increase in both measured MTE and calculated QE. The spectral response is significantly modified with emission shifted out into visible wavelengths, and the thermal floor not being reached

ISBN: 978-3-95450-231-8 ISSN: 2673-5490 doi: 10.18429/JACoW-IPAC2023-TUPA138

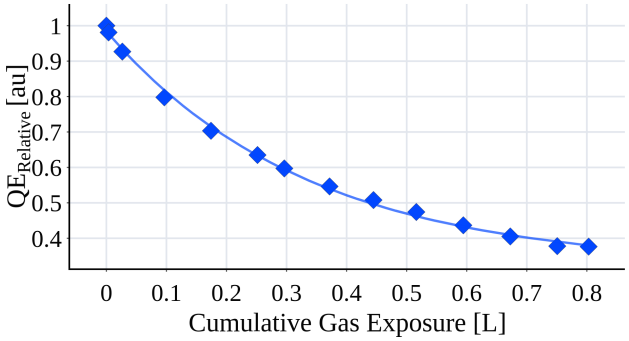

Figure 2: Relative QE values under illumination at 405 nm for Cs–implanted Cu subjected to progressive O_2 exposure.

until nearly 500 nm. The effect of the second implantation at 300 eV is less dramatic, though we can see a further small increase in MTE and an extension in the spectral response. An MTE estimate based on the Dowell–Schmerge model [1] using a work function of 2.14 eV for caesium [24] agrees well with the trend in the post–implantation data.

Fig. 2 shows how the second Cs–implanted Cu cathode responded when exposed to progressive degradation by O_2. We saw the QE fall by more than 60% due to the cumulative exposure of only 0.8 Langmuir (L) of O_2 where 1 L is equivalent to a gas exposure of 1.33 mbar·s. This demonstrates a level of robustness around 10 times better than activated GaAs [8], but the Cs–implanted complex is clearly much less robust than the bare polycrystalline Cu surface. Other work has shown a QE reduction of only 6% for polycrystalline Cu on exposure to 100 L of O_2 [23]. This implies that the Cs is very much confined to the surface of the Cu puck, with very little penetration into the bulk.

We measured QE at 405 nm in the PPF, obtaining a level of 0.012% after the first ion implantation, rising to around 0.023% after the second implantation. When measured later at 266 nm in the Multiprobe, we obtained 0.31%. Using the relative QE approach developed for TESS [22] and fitting this curve to the measured value at 405 nm, we reach a calculated QE at 266 nm of 0.58%, as shown in Fig. 1. There is a factor of less than 2 between the calculated QE value and the actual measured QE value at 266 nm. We consider this level of agreement to be good given that the actual measurement at 266 nm was made considerably later than the initial 405 nm measurement, and following transfer using our vacuum suitcase to a different chamber with a poorer base vacuum level. Furthermore, Fig. 1 shows that the QE at 266 nm of the Cs–implanted Cu is > 0.45% which is significantly more than a high–performing bare Cu cathode which typically exhibits a QE in the region of 10^{-2}% – 10^{-3}%.

Table 1: Summary of Measured Work Function Following Annealing for 1 Hour at Progressively–Increased Temperature

Annealing Temperature [°C]	200	300	400	500
Work Function, ϕ [eV]	2.1	2.6	3.8	4.8

The work function (ϕ) was measured and its dependence on temperature investigated. The data in Table 1 shows a clear reduction in ϕ due to Cs implantation, to a level close to the published value [24], with a step–wise increase in ϕ as the sample is heated and Cs progressively desorbed. We see ϕ = 4.8 eV at 500 °C which is typical for polycrystalline Cu [24]. This again implies that the Cs is confined very much to the Cu surface, and is not very deeply implanted.

Post–implantation surface roughness was measured ex–vacuum at 16 different positions using a MicroXAM interferometer. We found roughness levels in the range 9.1 ± 1.5 nm, which is in the same range as that previously measured in the Multiprobe by STM on the freshly–cleaned Cu photocathode sample 'pucks'. This indicates that Cs ion implantation at these energies does not affect surface roughness.

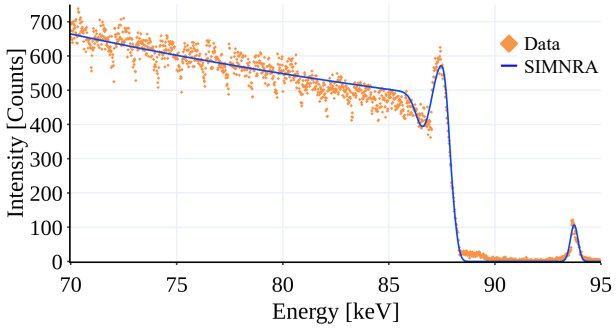

Figure 3: MEIS Data for Cu implanted with Cs ions at 500 eV indicating that the Cs is predominantly at the surface.

Fig. 3 shows preliminary results using the MEIS technique [25] with 100 keV H^+ ions. This data was analysed with SIMNRA [26] and indicates that the Cs is predominately located at the Cu surface, with a low coverage of around 0.13 monolayers in total. Only a small proportion of the Cs ions penetrate any distance into the Cu bulk, therefore the Cs remains chemically exposed.

CONCLUSION

Our work has shown the potential to create high QE low roughness photoemissive surfaces through Cs ion implantation, though with high levels of MTE and low levels of robustness. Further work is needed involving higher implantation energies to establish if sub–surface Cs exhibits improved emission and operational properties. The use of a protective layer such as graphene or an ultra–thin oxide film may also be beneficial.

ACKNOWLEDGEMENTS

The authors gratefully acknowledge funding from the *STFC Doctoral Training Studentship* and access to the Medium Energy Ion Scattering facility (MEIS) at the University of Huddersfield in delivering this work. We also thank Chris Benjamin and Hugh Churn for their preparation of the Cu substrates and assistance at the MEIS facility.

ISBN: 978-3-95450-231-8 ISSN: 2673-5490 doi: 10.18429/JACoW-IPAC2023-TUPA138

REFERENCES

[1] D. H. Dowell and J. F. Schmerge, "Quantum efficiency and thermal emittance of metal photocathodes", *Phys. Rev. Spec. Top. Accel Beams*, vol. 12, p. 074201, 2009. doi:10.1103/PhysRevSTAB.12.074201

[2] P. Saha *et al.*, "Theory of photoemission from cathodes with disordered surfaces", *J. Appl. Phys.*, vol. 133, p. 053102, 2023. doi:10.1063/5.0135629

[3] R. Akre *et al.*, "Commissioning the Linac Coherent Light Source injector", *Phys. Rev. Spec. Top. Accel. Beams*, vol. 11, p. 030703, 2008. doi:10.1103/PhysRevSTAB.11.030703

[4] E. Prat, S. Bettoni, H-H. Braun, R. Ganter, and T. Schietinger, "Measurements of copper and cesium telluride cathodes in a radio-frequency photoinjector", *Phys. Rev. Spec. Top. Accel. Beams*, vol. 18, p. 043401, 2015. doi:10.1103/PhysRevSTAB.18.043401

[5] D. Angal-Kalinin *et al.*, "Commissioning of Front End of CLARA Facility at Daresbury Laboratory", in *Proc. IPAC'18*, Vancouver, Canada, Apr.-May 2018, pp. 4426–4429. doi:10.18429/JACoW-IPAC2018-THPMK059

[6] C. Bates, Jr. *et al.*, "X-ray photoemission studies of superficially oxidized cesium antimonide photoemitters ", *Appl. Phys. Lett.*, vol. 38, pp. 387–389, 1981. doi:10.1063/1.92348

[7] A. di Bona *et al.*, "Auger and x-ray photoemission spectroscopy study on Cs2Te photocathodes", *J. Appl. Phys.*, vol. 80, p. 3024, 1996. doi:10.1063/1.363161

[8] N. Chanlek *et al.*, "The degradation of quantum efficiency in negative electron affinity GaAs photocathodes under gas exposure", *J. Phys. D: Appl. Phys.*, vol. 47, p. 055110, 2014. doi:10.1088/0022-3727/47/5/055110

[9] V. Pavlenko *et al.*, "Kinetics of alkali-based photocathode degradation", *AIP Adv.*, vol. 6, p. 115008 2016. doi:10.1063/1.4967349

[10] L. A. J. Soomary, L. B. Jones, T. C. Q. Noakes, and C. P. Welsch, "Controlled Degradation by Oxygen Exposure in the Performance of a Ag (100) Single-Crystal Photocathode", in *Proc. IPAC'21*, Campinas, Brazil, May 2021, pp. 2856–2859. doi:10.18429/JACoW-IPAC2021-WEPAB111

[11] R. K. Li *et al.*, "Surface-Plasmon Resonance-Enhanced Multiphoton Emission of High-Brightness Electron Beams from a Nanostructured Copper Cathode", *Phys. Rev. Lett.*, vol. 110, p. 074801, 2013. doi:10.1103/PhysRevLett.110.074801

[12] C. Benjamin *et al.*, "Photocathode performance characterisation of ultra-thin MgO films on polycrystalline copper", *J. Phys. Conf. Ser.*, vol. 2420, p. 012032, 2023. doi:10.1088/1742-6596/2420/1/012032

[13] L. Guo *et al.*, "Rugged bialkali photocathodes encapsulated with graphene and thin metal film", *Sci. Rep.*, vol. 13, p. 2412, 2023. doi:10.1038/s41598-023-29374-6

[14] J. Maxson, P. Musumeci, L. Cultrera, S. Karkare, and H. Padmore, "Ultrafast laser pulse heating of metallic photocathodes and its contribution to intrinsic emittance", *Nucl. Instrum. Meth. Phys. Res. Sect. A*, vol. 865, pp. 99–104, 2017. doi:10.1016/j.nima.2016.08.032

[15] J. Maxson, H. Lee, A.C. Bartnik, J. Kiefer, and I. Bazarov, "Adaptive electron beam shaping using a photoemission gun and spatial light modulator", *Phys. Rev. ST Accel. Beams*, vol. 18, p. 023401, 2015. doi:10.1103/PhysRevSTAB.18.023401

[16] K. Zhao, C. Chen, R. Geng, J. Yu, and B. Zhang, "Feasibility Study of Ion Implanted Photocathode for High-Brightness Injector", in *Proc. LINAC'94*, Tsukuba, Japan, Aug. 1994, paper TU–21, pp. 413–414.

[17] K. Zhao *et al.*, "Researches on new photocathode for RF electron gun", *Nucl. Instrum. Meth. Phys. Res. Sect. A*, vol. 445, pp. 394–398, 2000. doi:10.1016/S0168-9002(00)00090-5

[18] Y. X. Tang *et al.*, "Experimental study of new-type Cs+ ion-implanted Mg photocathode", *Acta Physica Sinica*, vol. 49, pp. 1002–1005, (2000. doi:10.7498/aps.49.1002

[19] Omicron Spare Parts Catalogue SPM, v.2.4, 2019, Part # S220601-S, https://scientaomicron.com/Services-Support/SpareParts-Catalogues/Spare_Parts_Catalogue_S_SPM_07_2019.pdf

[20] T. C. Q. Noakes, B. L. Militsyn, R. Valizadeh, K. J. Middleman, A. N. Hannahn and L. B. Jones, "Commissioning of the SAPI for operation with metal photocathodes", CERN, Geneva, Switzerland, CERN-ACC-2014-0039, 2014. https://cds.cern.ch/record/001664319

[21] B. L. Militsyn *et al.*, "First Results from III-V Photocathode Preparation Facility for the ALICE ERL Photoinjector", in *Proc. IPAC'10*, Kyoto, Japan, May 2010, paper TUPE095, pp. 2347–2349.

[22] L. B. Jones *et al.*, "The measurement of photocathode transverse energy distribution curves (TEDC) using the transverse energy spread spectrometer (TESS) experimental system", *Rev. Sci. Instrum.*, vol. 93, p. 113314, 2022. doi:10.1063/5.0109053

[23] L. A. J. Soomary, University of Liverpool, Ph.D. Thesis (submitted Apr '23).

[24] H. B. Michaelson, "The work function of the elements and its periodicity", *J. Appl. Phys.*, vol. 48, p. 4729, 1977. doi:10.1063/1.323539

[25] R. J. Barlow, "The UK MEIS Facility : A New Future", in *Proc. IPAC'12*, New Orleans, LA, USA, May 2012, paper TH-PPR075, pp. 4151–4153.

[26] M. Mayer, SIMNRA, Max-Planck-Institut für Plasmaphysik. https://mam.home.ipp.mpg.de/.